Marine teleost ortholog of catalase from rock bream (Oplegnathus fasciatus): Molecular perspectives from genomic organization to enzymatic behavior with respect to its potent antio...

Article *in* Fish & Shellfish Immunology · July 2013

DOI: 10.1016/j.fsi.2013.07.013 · Source: PubMed

CITATIONS
6

READS
162

10 authors, including:

Don Anushka Sandaruwan Elvitigala
University of Colombo
63 PUBLICATIONS **240** CITATIONS
SEE PROFILE

H.K. Ajith Premachandra
University of Peradeniya
52 PUBLICATIONS **176** CITATIONS
SEE PROFILE

Ilson Whang
150 PUBLICATIONS **2,292** CITATIONS
SEE PROFILE

Thanthrige Thiunuwan Priyathilaka
University of Wisconsin–Madison
35 PUBLICATIONS **102** CITATIONS
SEE PROFILE

Some of the authors of this publication are also working on these related projects:

Teleost immuno-genetics View project

Development of Breeding Program for Abalone Golden Seed View project

Fish & Shellfish Immunology 35 (2013) 1086–1096

Contents lists available at ScienceDirect

Fish & Shellfish Immunology

journal homepage: www.elsevier.com/locate/fsi

Marine teleost ortholog of catalase from rock bream (*Oplegnathus fasciatus*): Molecular perspectives from genomic organization to enzymatic behavior with respect to its potent antioxidant properties

Don Anushka Sandaruwan Elvitigala [a], H.K.A. Premachandra [a], Ilson Whang [a], Thanthrige Thiunuwan Priyathilaka [a], Eunmi Kim [b], Bong-Soo Lim [c], Hyung-Bok Jung [c], Sang-Yeob Yeo [d], Hae-Chul Park [b,**], Jehee Lee [a,c,*]

[a] Department of Marine Life Sciences, School of Marine Biomedical Sciences, Jeju National University, Jeju Self-Governing Province 690-756, Republic of Korea
[b] Graduate School of Medicine, Korea University, Ansan, Gyeonggido 425-707, Republic of Korea
[c] Marine and Environmental Institute, Jeju National University, Jeju Special Self-Governing Province 690-814, Republic of Korea
[d] Department of Biotechnology, Division of Applied Chemistry & Biotechnology, Hanbat National University, Daejeon 305-719, Republic of Korea

ARTICLE INFO

Article history:
Received 14 March 2013
Received in revised form
22 June 2013
Accepted 9 July 2013
Available online 17 July 2013

Keywords:
Catalase
Rock bream
Genomic organization
Transcriptional profiling
Peroxidase activity

ABSTRACT

Catalases are well known antioxidant enzymes that can mainly dismutate hydrogen peroxide into water and oxygen in order to prevent oxidative stress. The complete genomic DNA (gDNA) sequence of the catalase gene from rock bream (*Oplegnathus fasciatus*) was identified from our custom-constructed BAC genomic DNA library and designated as *RbCat*. *RbCat* consists of 13 exons, separated by 12 introns, within a 13,722-bp gDNA sequence. The complete cDNA sequence (3303 bp) of *RbCat* is comprised of a 1581-bp coding region, encoding a peptide of 527 amino acids (aa) in length, with a predicted molecular mass of 60 kDa and a theoretical isoelectric point of 8.34. The anticipated promoter region of *RbCat* contains several transcription factor-binding sites, including sites that bind with immune- and antioxidant-responsive signaling molecules, suggesting its substantial transcriptional regulation. RbCat resembles the typical catalase family signature, i.e., it is composed of the catalase proximal active site motif along with a catalase proximal heme-ligand signature motif and shares great homology with its fish counterparts. According to multiple sequence alignment, functionally important amino acids present in RbCat were thoroughly conserved among its vertebrate counterparts. Phylogenetic analysis revealed that RbCat evolved from a vertebrate origin, and further positioned it in the fish clade. Recombinant RbCat had noticeable peroxidase activity against its substrate, hydrogen peroxide, in a dose-dependent manner. However, it demonstrated substantial peroxidase activity within a broad range of temperatures and pH values. Constitutive RbCat mRNA expression of different magnitudes was detected in a tissue-specific manner, suggesting its diverse role in physiology with respect to the tissue type. Moreover, immune challenge experiments using *Edwardsiella tarda* and rock bream iridovirus (RBIV) as live pathogens and polyinosinic:polycytidylic acid and lipopolysaccharide as mitogens revealed that the transcription of RbCat can be modulated by immune stimulation. Collectively, the results obtained in this study suggest that RbCat can function as a potent antioxidant enzyme in rock bream and may play a role in post-immune responses with respect to its peroxidase activity.

1. Introduction

Aerobic respiration is a key metabolic mechanism to gain chemical energy in biological systems, which directly contributes to cellular functions and survival of organisms. However, as a result of this biological process, toxic molecules, known as reactive oxygen species (ROS), are released as byproducts, which represent a risk to the cellular environments leading to grievous consequences. ROS is

* Corresponding author. Marine Molecular Genetics Lab, Department of Marine Life Sciences, College of Ocean Science, Jeju National University, 66 Jejudaehakno, Ara-Dong, Jeju 690-756, Republic of Korea. Tel.: +82 64 754 3472; fax: +82 64 756 3493.
** Corresponding author. Tel.: +82 31 412 6712; fax: +82 31 412 6729.
E-mail addresses: hcpark67@korea.ac.kr (H.-C. Park), jehee@jejunu.ac.kr, jeheedaum@hanmail.net (J. Lee).

1050-4648/$ – see front matter © 2013 Elsevier Ltd. All rights reserved.
http://dx.doi.org/10.1016/j.fsi.2013.07.013

a collective term, used to designate both oxygen radicals and certain oxidizing agents that are easily converted into radicals, including singlet oxygens ($^1O_2$), superoxide anions (O_2^-), hydrogen peroxides (H_2O_2), and hydroxyl radicals ($^{\bullet}OH$) [1,2]. ROS generation is known to be particularly stimulated under pathogenic conditions upon microbial invasions, through identification of different molecular patterns of these invaders by pathogen recognition receptors such as NLRX1 [3–5]. Therefore, production of ROS is considered as one of the early responses in host innate immunity that is highly toxic to the invading pathogens. As a consequence of pathogenic infection, phagocytosis in the host organism is activated, consuming excessive amounts of oxygen to facilitate changes in cellular environments, leading to respiratory burst. The major result of this process is the generation of ROS under catalysis of NADPH oxidase complexes [5,6]. In addition to the direct harm to the invading pathogens, it can also act as a secondary signaling molecule to induce inflammatory and immune responses. According to previous literature, ROS are able to induce a wide array of signaling networks, including innate immune pathways, enhancing the expression levels of nuclear factor kappa B and mitogen-activated protein kinase, further mediating cell growth and apoptosis [7–9].

The extreme condition of excessive production of ROS, which leads to the accumulation of higher levels of oxygen radicals, is known as oxidative stress. This condition may potentiate cellular responses such as apoptosis, tumorigenesis, and immune responses [7,10,11]. On one hand, exerting immune responses against invaders are considered as desirable features of ROS. On the other hand, collectively, damages to the cell membranes due to lipid peroxidation, oxidative damage to proteins, generation of mutations in the DNA, and activation of pro-cell death factors are considered as major deleterious effects of the generated ROS in cellular environments, rendering them as double-edged swords [1]. Moreover, accumulation of ROS in cellular environment is also known to evoke immune dysfunction [12].

Antioxidants have been identified as potent players in counterbalancing the produced ROS in cellular environments, while protecting the cells from the grievous effects of oxidative stress, especially converting them to less toxic products. Enzymatic antioxidants, including catalase, superoxide dismutase, glutathione peroxidase, thioredoxin, thioredoxin reductase, and peroxiredoxins [2] as well as non-enzymatic antioxidants, including glutathione, vitamins A, E, and C [13] are known to play a crucial role in preventing oxidative stress.

Among the above-mentioned antioxidant enzymes, catalases play a major role in the detoxification of H_2O_2 by dismutating it into water and oxygen [2], while maintaining the correct balance of *in-vivo* H_2O_2 generation and decomposition which in turn plays an important role in innate immunity [14]. There are 2 basic types of catalases found in living organisms. They are classical Fe heme enzymes, characterized as a small group of "manganese enzymes," and "catalase peroxidases," which are known to be heme enzymes that also contain a covalent triplet of distal side chains, and catalyze peroxidatic as well as catalytic reactions using different mechanisms, compared to classical heme enzymes [15]. In addition to the dismutation of peroxides, catalases can catalyze some detoxification events of subsidiary molecules in organisms, including phenol, methanol, ethanol, and nitrites [16]. Even though catalases are ubiquitous proteins both in prokaryotes and eukaryotes [17,18], much information about their structure and regulation at gene and protein levels have only been accumulated in mammals [19,20], plants [21], and bacteria [22]. Catalases have a tetrameric structure with 4 subunits of 50–60 kDa, harboring a single heme group and NADPH molecule per every subunit. NADPH is bound on the surface of each monomer by 12 amino acid residues, protecting the enzyme from oxidation by its substrate H_2O_2 [23,24].

With regard to teleosts, catalase was completely characterized only in zebrafish, reflecting the scarce information on catalase from fish origin [25,26]. However, catalase has been extensively characterized for many invertebrate species, including mollusks such as disk abalone [27], Zhikong scallop [28], and pearl oyster [29] as well as crustaceans, e.g., shrimps [30].

Rock bream is consumed as a comestible in many areas of the world, including eastern and northeastern countries such as China, Japan, and Korea, mostly through cultivating them as a mariculture fish species. Therefore, the yield of this aqua-crop has become one of the critical factors to maintain a positive economic status in the countries mentioned above. However, environmental stress conditions, including pathogen infections, have seriously affected the survival of this marine creature, being responsible for its significant mortality rate [31–33]. Stress conditions such as oxidative stress are known to be involved in damaging the immune system in fish species and thus, increase the susceptibility to various pathogenic infections [34]. Therefore, exploration of molecular level information of antioxidant enzymes such as catalase will be a productive primary approach of finding solutions to decrease the mortality rate of cultivated rock bream.

In this study, an ortholog of a catalase from rock bream (*Oplegnathus fasciatus*) was characterized at the genomic, mRNA, as well as protein level; the antioxidant activity of its purified recombinant protein against H_2O_2 was demonstrated under different temperature and pH conditions. Moreover, we investigated variations of the transcriptional profiles upon exposure to different immune stimulants, i.e., *Edwardsiella tarda* (*E. tarda*) and rock bream iridovirus (RBIV) as live pathogens and polyinosinic:polycytidylic acid (poly I:C) and lipopolysaccharide (LPS) as mitogens.

2. Materials and methods

2.1. Identification of the complete cDNA sequence of RbCat

The complete cDNA sequence of the catalase gene (*RbCat* – Contig number – 02273) of rock bream was identified using the Basic Local Alignment Search Tool (BLAST) algorithm (http://blast.ncbi.nlm.nih.gov/Blast.cgi) from a previously established cDNA sequence database [35].

2.2. Identification of the complete genomic sequence of RbCat

A random-shear bacterial artificial chromosome (BAC) library of rock bream genomic DNA was custom-constructed (Lucigen, USA) and used to screen the *RbCat* gene, according to pooling and super pooling strategies, implemented through polymerase chain reaction (PCR), using a sequence-specific primer pair, RbCat-qF and RbCat-qR (Table 1), as described previously [36]. The primers were designed according to the previously identified *RbCat* (Section 2.1) cDNA sequence. The PCR was conducted in a TaKaRa thermal cycler in a total volume of 20 μL with 0.5 U of Ex Taq polymerase (TaKaRa, Japan), 2 μL of 10 × Ex Taq buffer, 1.6 μL of 2.5 mM dNTPs, 75 ng of template, and 10 pmol of each primer. The reaction was carried out with an initial incubation at 94 °C, followed by 35 cycles of 94 °C for 30 s, 58 °C for 30 s, and 72 °C for 30 s. The PCR products were analyzed on a 1.5% agarose gel and the correct location of the BAC clone was detected according to the appearance of the corresponding band. Subsequently, the detected clone was sequenced (GS-FLX™) in order to obtain the genomic DNA sequence of the *RbCat* gene. The open reading frame of *RbCat* was identified by using the NCBI-BLAST algorithm (http://www.ncbi.nlm.nih.gov/BLAST) from the above-confirmed genomic DNA sequence. The

Table 1
Oligomers used in this study.

Name	Purpose	Sequence (5′ → 3′)
RbCat -qF	BAC library screening and qRT-PCR of *RbCat*	TGG CAGGTTACATGGTACGTTTAATGC T
RbCat -qR	BAC library screening and qRT-PCR of *RbCat*	TTGTGGGCGTCTGCATATCATGAAGA
RbCat -F	ORF amplification (*Eco*RI)	GAGAGAgaattcATGGCTGACAACAGAGGCAAAGCTAC
RbCat -R	ORF amplification (*Hin*dIII)	GAGAGAaagcttTCACAT CTTGGAGGACGCAGCG
Rb-βF	qRT-PCR for rock bream β-actin gene	TCATCACCATCGGCAATGAGAGGT
Rb-βR	qRT-PCR for rock bream β-actin gene	TGATGCTGTTGTAGGTGGTCTCGT

nucleotide sequence of the *RbCat* gene was deposited in GenBank under the accession number KC201280.

2.3. In-silico characterization of RbCat

Orthologous sequences of RbCat were compared by using the BLAST search program. Pairwise sequence alignment (http://www.Ebi.ac.uk/Tools/emboss/align) and multiple sequence alignment (http://www.Ebi.ac.uk/Tools/clustalw2) were performed using the EMBOSS Needle and ClustalW2 programs, respectively. The phylogenetic relationship of RbCat was determined by using the neighbor-joining method and Molecular Evolutionary Genetics Analysis (MEGA) software version 4 [37]. Protein domains were predicted by using the ExPASy prosite database (http://prosite.expasy.org), MotifScan scanning algorithm (http://myhits.isb-sib.ch/cgi-bin/motif_scan), and the NCBI-CDS server [38]. Some properties of RbCat were determined by using the ExPASy ProtParam tool (http://web.expasy.org/protparam). Moreover, the tertiary structure of RbCat was predicted on the basis of the iterative assembly simulation strategy using the I-TASSER online server [39,40] and three-dimensional (3D) images were generated using RasMol 2.7.5.2 software [41].

The genomic sequence of RbCat, identified from the BAC clone, was used to identify the genomic architecture revealing the exon–intron arrangement and tentatively derive the promoter region, along with potential transcriptional factor-binding sites. The transcription initiation site (TIS) was predicted using the neural network promoter prediction tool from the Berkeley Drosophila Genome Project [42], and potential *cis*-acting elements around 1 kb upstream of TIS was detected using TFSEARCH ver.1.3 and Alibaba 2.1 software.

2.4. Expression and purification of recombinant RbCat (rRbCat)

Recombinant RbCat was expressed as a fusion protein with the maltose binding protein (MBP) and purified as described previously, with some modifications [43]. Briefly, the open reading frame of the *RbCat* gene was amplified using the sequence-specific primers RbCat-F and RbCat-R with restriction enzyme sites for *Eco*RI and *Hin*dIII, respectively (Table 1). The PCR was performed in a TaKaRa thermal cycler in a total volume of 50 μL with 5 U of Ex Taq polymerase (TaKaRa, Japan), 5 μL of 10 × Ex Taq buffer, 8 μL of 2.5 mM dNTPs, 80 ng of template, and 20 pmol of each primer. The reaction was carried out at 94 °C for 30 s, 58 °C for 30 s, and 72 °C for 1 min, followed by a final extension step at 72 °C for 5 min. The PCR product (~1.6 kbp) was resolved on a 1% agarose gel, excised, and purified using the Accuprep™ gel purification kit (Bioneer Co., Korea). The digested pMAL-c2X vector (150 ng) and PCR product (180 ng) were ligated using Mighty Mix (7.5 μL; TaKaRa) at 4 °C overnight. The ligated pMAL-c2X/RbCat product was transformed into DH5α cells and sequenced. The Sequence-confirmed recombinant expression plasmid was transformed into *Escherichia coli* BL21 (DE3) competent cells. The rRbCat protein was overexpressed using isopropyl-β-galactopyranoside (IPTG, 1 mM final concentration) at 20 °C for 8 h, after which the protein was purified using the pMAL protein fusion and purification system (New England Biolabs, USA). The purified protein was eluted with elution buffer (10 mM maltose) and the concentration was determined by using the Bradford method; bovine serum albumin served as standard [44]. The rRbCat samples collected from different purification steps were analyzed on 12% sodium dodecyl sulfate-polyacrylamide gel electrophoresis (SDS-PAGE) under reduced conditions, with a standard molecular weight marker (Enzynomics-Korea). The gel was stained with 0.05% Coomassie blue R-250, followed by a standard destaining procedure.

2.5. Analysis of antioxidant activity of rRbCat

In order to functionally characterize rRbCat, the peroxidase activity of rRbCat fusion protein was analyzed using a gradient of different concentrations of the protein, according to a previous report, with some modifications [45]. Briefly, 50 μL rRbCat (containing different amounts of protein at each time) was dissolved in 70 μL of phosphate buffer (0.05 M, pH 5) with 20 μL of 10 mM H_2O_2 in a 96-microwell plate and incubated at 37 °C for 5 min. Subsequently, 30 μL of 2,2′-azino-bis(3-ethylbenzothiazoline-6-sulphonic acid) (ABTS) and 30 μL of peroxidase (1 U/mL) were added to the mixture and the mixture was again incubated at 37 °C for 10 min. As a result of the incubation of ABTS with peroxidase, a blue-green colored cationic radical of ABTS is produced, which can be spectrophotometrically detected at 405 nm. The enzyme assay was performed in triplicates and the mean values were considered for the final calculation. One unit of catalase activity was defined as the amount of catalase required to decompose 1.0 μmol of H_2O_2 per min under the applied assay conditions. In each assay, MBP was used as a control to determine the effect of fusion on the activity of rRbCat. Blanks were prepared in a similar manner without adding the protein, while a constant volume was maintained by increasing the volume of phosphate buffer accordingly.

2.6. Evaluation of the biochemical properties of rRbCat

To characterize the enzymatic activity of rRbCat with respect to the reaction temperature and pH, the antioxidant assay used for RbCat, described in the above section, was carried out using 25 μg of protein under different temperature and pH conditions. The activity was calculated as percentage activity, considering the difference in the optical density (OD) at 405 nm of the corresponding reaction mixtures of sample and negative control (without protein), relative to the OD_{405} of the negative control. In order to analyze the temperature dependency, the reaction was performed at temperatures ranging from 10 °C to 80 °C in 10 °C intervals. However, instead of 40 °C, 37 °C was used, since it was the previously mentioned optimal temperature for the reaction in the standard procedure. Similarly, the standard peroxidase reaction catalyzed by rRbCat was employed under different pH conditions. A pH gradient was obtained using acetate, phosphate, and glycine–NaOH buffers of different pH values, ranging from pH 4.5 to 9.5 in 0.5 pH intervals.

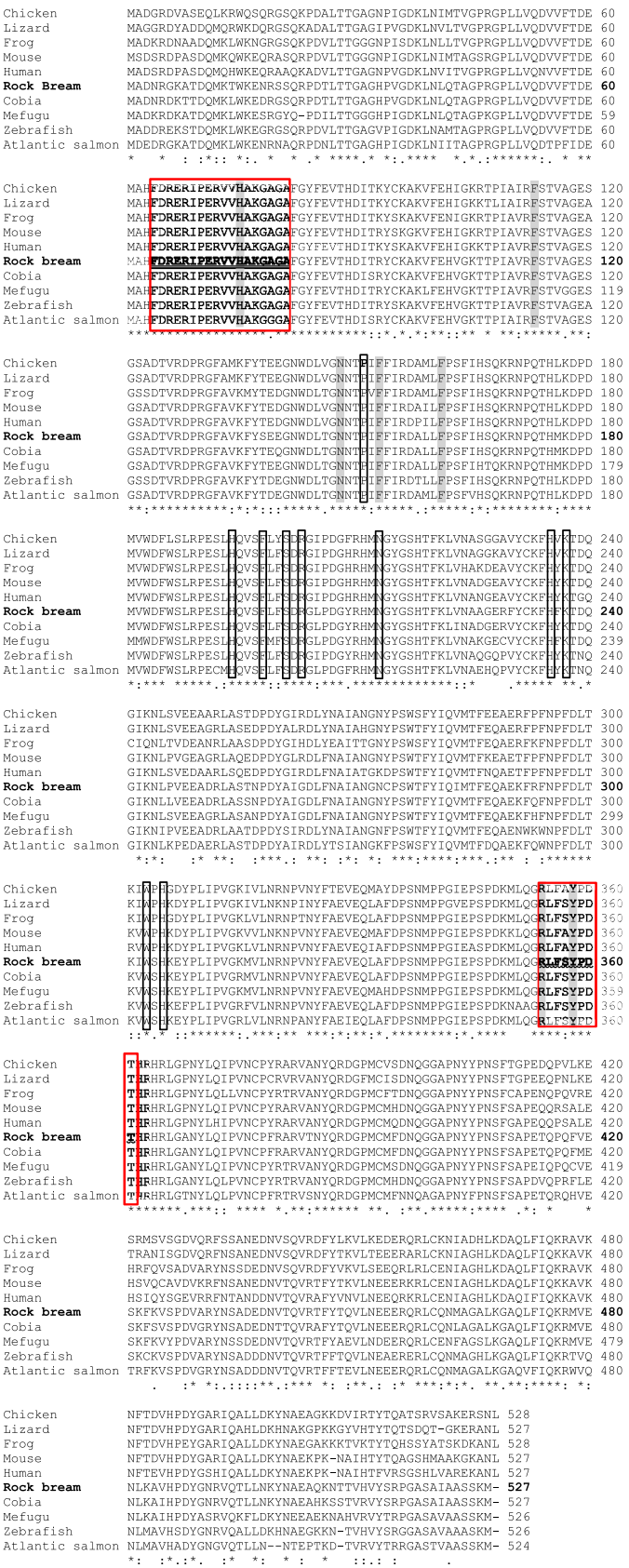

Fig. 1. Multiple sequence alignment of rock bream catalase (RbCat) with its vertebrate counterparts. Sequence alignment was obtained using Clustal-W method. The conserved catalase proximal active site motifs (64–81) and proximal heme-ligand signature motifs (354–361) among the species were denoted by red color boxes, while the corresponding sequence in RbCat is indicated using double underlining and pattern underlining, respectively. Conserved heme-binding sites were shaded in gray color and NADPH-binding sites were boxed separately. (For interpretation of the references to color in this figure legend, the reader is referred to the web version of this article.)

2.7. Experimental fish and tissue collection

Rock breams, with an average body weight of 30 g, were obtained from the Jeju Special Self-Governing Province Ocean and Fisheries Research Institute (Jeju, Republic of Korea). The fish were maintained in a controlled environment at 22–24 °C and acclimatized for 1 week prior to experimentation. During this period fish were daily fed with commercially available feed. Whole blood (~1 mL/fish) was collected from the caudal fin using a sterilized syringe, and the sample was immediately centrifuged at 3000× *g* for 10 min at 4 °C to separate the blood cells from the plasma. The collected cells were snap-frozen in liquid nitrogen. Meanwhile, the sampled fish was dissected and gill, liver, skin, spleen, head kidney, kidney, skin, muscle, brain, intestine, and heart were excised, immediately snap-frozen in liquid nitrogen, and stored at −80 °C until use for total RNA extraction.

2.8. Immune challenge experiments

In order to determine changes in the transcription of RbCat upon live pathogen infection and pathogen derived mitogen stimulation, *E. tarda* and RBIV along with LPS, and poly I:C were employed as immune stimulants in time-course immune challenge experiments, respectively. Blood cells were collected as described in Section 2.7. The immune challenge experiments were carried out as described previously; tissues were collected from at least 3 animals from each challenge group at each time point [46].

2.9. Total RNA extraction and cDNA synthesis

Total RNA was extracted by using Tri Reagent™ (Sigma) from blood, gill, liver, spleen, head kidney, kidney, skin, muscle, brain, intestine, and heart from healthy rock breams along with blood cells from immune-challenged animals. Subsequently, cDNA was synthesized from each set of RNA as described previously [35].

2.10. RbCat transcriptional analysis by reverse transcription PCR followed by quantitative real time (qRT)-PCR

qRT-PCR was used to analyze the expression levels of *RbCat* in all tissues mentioned in Section 2.9, collected from healthy animals and the temporal expression of *RbCat* in blood. Subsequent to the cDNA synthesis using the total RNA extracted from each tissue, qRT-PCR was carried out using the thermal cycler Dice™ Real Time System (TP800; TaKaRa, Japan). The reaction was conducted in a 15 μL reaction volume containing 4 μL of diluted cDNA from each tissue, 7.5 μL of 2 × TaKaRa Ex Taq™, SYBR premix, 0.6 μL of each primer (RbCat-qF and RbCat-qR; Table 1), and 2.3 μL of ddH_2O. The qRT-PCR was performed under the following conditions: 95 °C for 10 s, followed by 35 cycles of 95 °C for 5 s, 58 °C for 10 s, and 72 °C for 20 s, and a final cycle of 95 °C for 15 s, 60 °C for 30 s, and 95 °C for 15 s. The base line was set automatically by the Dice™ Real Time System software (version 2.00). RbCat expression was determined by applying the Livak ($2^{-\Delta\Delta CT}$) method [47]. The same qRT-PCR cycle profile was used for the internal control gene, rock bream β-actin (GenBank ID: FJ975145), using respective oligomers (Table 1). All data are presented as mean ± standard deviation (SD) of the relative mRNA expression of 3 replicates. To determine

Table 2
Percentage similarity and identity values of RbCat with its orthologs. Accession numbers of chicken and anole lizard catalases protein sequences were obtained from Ensemble and EMBL databases, respectively, and the remaining ones were extracted from NCBI-GenBank sequence database.

Species	Accession number	Amino acids	Identity (%)	Similarity (%)
1. *Rachycentron canadum* (Cobia)	ACO07305	527	94.1	97.2
2. *Takifugu obscurus* (Mefugu)	ABV24056	526	89.4	93.7
3. *Kryptolebias marmoratus* (Mangrove rivulus)	ABW88893	514	88.2	93.4
4. *Danio rerio* (Zebrafish)	AAF89686	526	86.3	93.5
5. *Salmo salar* (Atlantic salmon)	ACN11170	524	83.9	92.6
6. *Mus musculus* (Mouse)	AAA66054	527	80.3	88.7
7. *Canis lupus familiaris* (Dog)	BAB20764	527	80.3	88.5
8. *Sus scrofa* (Pig)	NP999466	527	80.5	87.9
9. *Homo sapiens* (Human)	AAK29181	527	77.3	86.7
10. *Xenopus laevis* (Frog)	ABK62836	528	77.5	86.6
11. *Gallus gallus* (Chicken)	ENSGALP00000023319	528	78.1	87.7
12. *Anolis carolinensis* (Anole lizard)	ENSACAP00000013065	527	77.8	86.7
13. *Chlamys farreri* (*Akazara scallop*)	ABI64115	507	66.2	78.6
14. *Fenneropenaeus chinensis* (Shrimp)	ABW82155	520	67.0	78.1
15. *Pinctada fucata* (Pearl oyster)	ADW08700	512	67.0	78.7
16. *Scylla paramamosain* (Crab)	ACX46120	517	67.3	78.8
17. *Anemonia viridis* (Sea anemone)	AAZ50618	509	67.9	78.0
18. *Eisenia fetida* (worm)	AEO50756	505	66.0	77.4

statistical significance ($P < 0.05$) between the experimental and control groups, a two-tailed paired *t*-test was carried out.

3. Results and discussion

3.1. Sequence characterization and phylogenetic relationship of RbCat

The complete cDNA sequence of *RbCat* consists of 3303 bp nucleotides, which comprises a 1581-bp coding sequence, encoding a peptide of 527 amino acids, a 293-bp 5′-untranslated region (5′-UTR), and a 1429-bp 3′-UTR. The predicted molecular mass of RbCat was around 60 kDa, complying with that of other known catalases [48], and the theoretical isoelectric point was 8.34. According to the *in-silico* predictions, RbCat resembled the typical catalase family signature, containing catalase proximal active site motif (64–81) and catalase proximal heme-ligand signature motif (354–361) (Fig. 1), which are known to be highly conserved motifs in most catalases [49]. In addition, well conserved potential heme-binding sites (H_{75}, F_{113}, N_{148}, F_{153}, F_{161}, R_{354}, Y_{358}) and NADPH-binding residues (P_{151}, H_{194}, F_{198}, S_{201}, R_{203}, N_{213}, H_{235}, K_{237}, W_{303}, H_{305}) were also present in the derived amino acid sequence of RbCat, as anticipated by NCBI-CDS server (Fig. 1). These binding sites render antioxidant protection from its substrate, H_2O_2, on the surface and within the enzyme [50].

According to the results from pair wise sequence alignment, RbCat shared greatest identity (94.1%) and similarity (97.2%) with its vertebrate counterpart from *Rachycentron canadum* (Cobia), whereas the lowest identity value (66%) and similarity value (77.4%) was shown with its invertebrate counterpart from *Eisenia fetida* (worm) (Table 2), validating RbCat as a vertebrate ortholog of catalases.

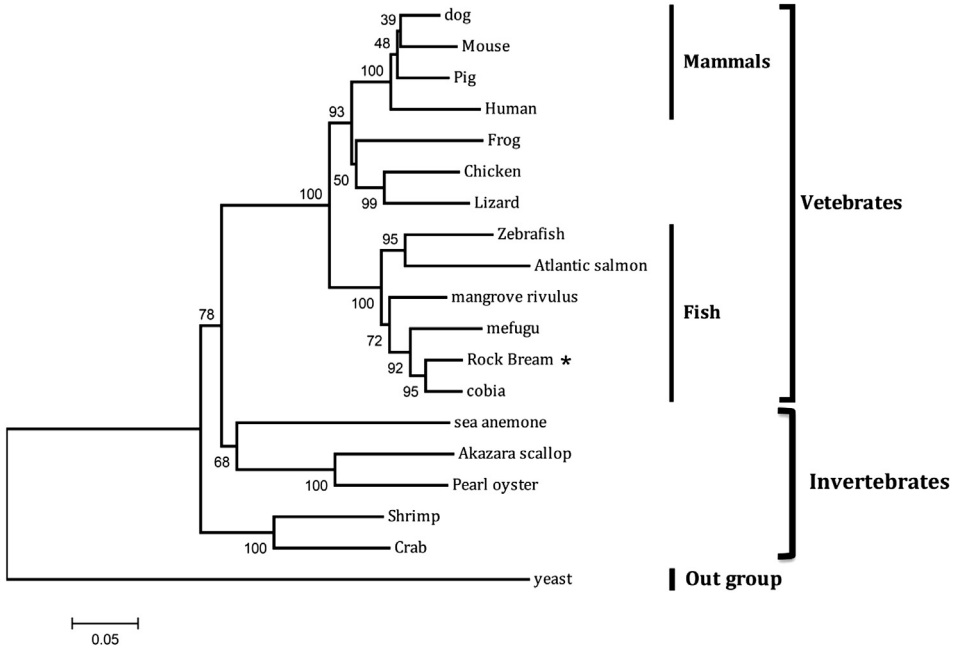

Fig. 2. Phylogenetic tree construct generated on the basis of ClustalW alignment of the deduced amino acid sequences of various catalase protein sequences, estimated by using the neighbor-joining method in MEGA version 4.0. Bootstrap values are shown on the lineages of the tree and NCBI and Ensemble accession numbers of the respective sequences are given in Table 2.

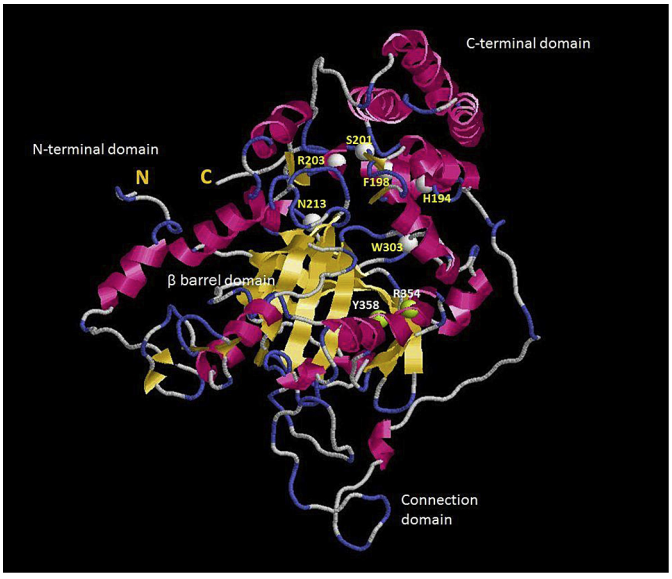

Fig. 3. Tertiary structure of rock bream catalase (RbCat) modeled according to the ab-initio strategy. Four conceptual domains of RbCat were labeled in the model. α-Helixes and β-strands are depicted in pink color and yellow color, respectively. Ash color spherical bulges represent some of the amino acid residues important in NADPH binding, whereas green color bulges represent the residues important in heme binding. N and C letters were used to indicate the amino and carboxyl terminal, respectively. (For interpretation of the references to color in this figure legend, the reader is referred to the web version of this article.)

In order to evaluate the evolutionary relationship of RbCat with its vertebrate and invertebrate counterparts, a phylogenetic analysis was carried out. As depicted in Fig. 2, there were 2 main independent clusters in the generated tree diagram as expected, vertebrates and invertebrates. Interestingly, RbCat was grouped in the vertebrate cluster, further subclustered into the fish clade, showing a close evolutionary proximity with the catalase counterpart of cobia fish, exhibiting a prominent boost trap value (95). This pattern of clustering indicates that RbCat evolved from a common vertebrate ancestral origin of catalases, further affirming its diversification from mammalian, avian, and amphibian counterparts.

3.2. Modeled tertiary structure of RbCat

In order to correlate the function of RbCat with its structural properties, the 3D structure of RbCat was modeled using the ab-initio protein prediction strategy. The model represented valuable information on the arrangement of its functionally important residues in 3D space. The top ten catalase template structures obtained from the Research Collaboratory for Structural Bioinformatics (RCSB) protein data bank exhibited 42%–78% identity with the query sequences, while normalized *Z*-scores of the threading alignment of each sequence exceeded 1 (3.39–4.47). These parameters, calculated by the server program, substantially affirm the reliability of the predicted model.

Resembling the tertiary structure of human catalase, four conceptual domains were identified in the generated model of RbCat. They were designated as N-terminal domain that forms an extended non-globular amino-terminal arm, C-terminal domain that bears four α-helices, anti-parallel octa-stranded β-barrel domain, and connection domain forming a folding loop (Fig. 3), validating RbCat as a novel counterpart of the human catalase enzyme [24]. Moreover, some of the amino acid residues present in the heme-binding sites (R_{354} and Y_{358}) and important in the NADPH-binding sites (H_{194}, F_{198}, S_{201}, R_{203}, N_{213}, W_{303}) and noticed in our generated model structure were compatible with those of the human catalase tertiary structure. This finding affirms the correct orientation of the 3D globular arrangement of RbCat with respect to its functional properties.

3.3. Genomic architecture and predicted core promoter region of *RbCat*

According to the canonical AG/exon/GT rule, the exon–intron organization of the *RbCat* gene in the identified BAC gDNA sequence was analyzed and compared with the derived complete cDNA sequence. The genomic structure revealed that RbCat consists of 13 exons, separated by 12 introns, with a genome length of 13,722 bp (Fig. 4). According to the comparison with its orthologs, the number and size of the exons (from the 3rd to 12th) of RbCat were found to be well conserved among all vertebrate species. The second exon is conserved among the majority, including the mammals considered in the comparison, rendering a greater potential of evolution through mechanisms such as alternative splicing [51,52], which

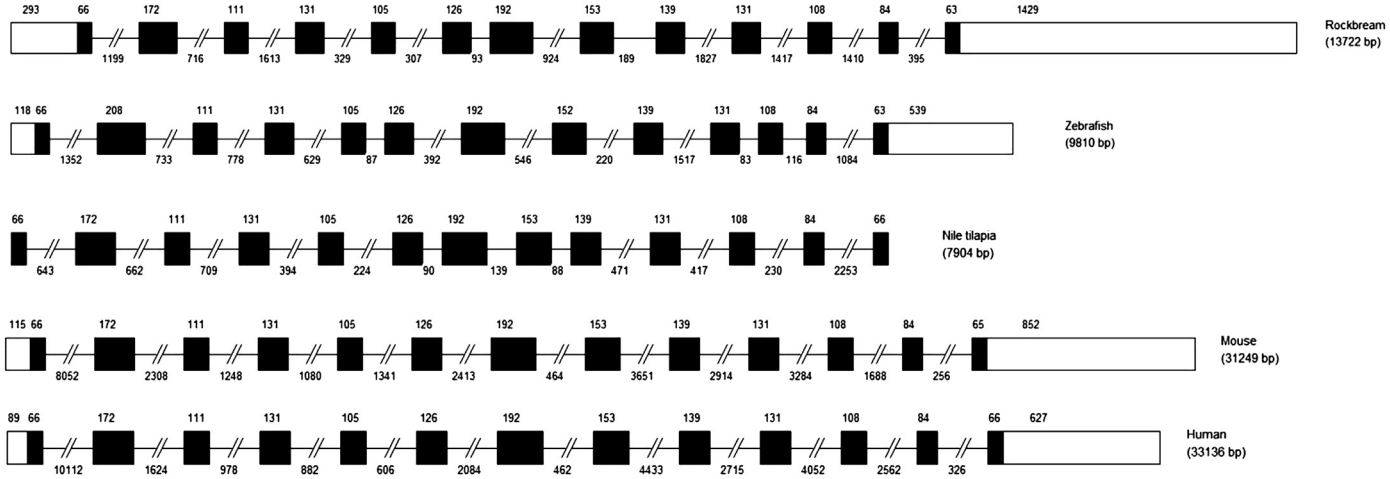

Fig. 4. Genomic organization of the catalase gene from different species. The exons and introns are indicated by boxes and solid lines, respectively. The sizes of exons are indicated above the exons and sizes of introns are indicated below the introns. Black regions represent the coding sequences whereas white regions represent untranslated regions. When representing introns, sequence regions larger than 100 bp are truncated by 2 inclined lines. NCBI-GenBank accession numbers of the genomic sequences of organisms used in the comparison are as follows: Zebrafish – NC007136, Nile tilapia – NT167433, Mouse – NC000068, Human – NG013339.

further supports the potential existence of different isoforms. Moreover, among the 3 fish species considered, rock bream exhibited eminent genomic length, possessing large exons at the beginning and end of the sequence.

According to the promoter prediction, the approximate 1-kbp region upstream from TIS consisted of several transcriptional factor-binding sites, including a TATA box and a CAAT box, reflecting the tight regulation of its transcription (Fig. 5). Most of the predicted *cis*-active sites coincided with the previously characterized promoters of different catalases from vertebrates, especially from mammals. Factors recognizing Sp1 and CCAAT sites were found to be strong regulators of catalase expression at the transcriptional level [53]; C/EBP-β was reported as a potent transcriptional regulator that can interact with corresponding binding regions of catalase promoters [54]. Catalase gene expression can also be regulated by the OCT-1 transcriptional factor, which is also present in the predicted RbCat promoter region. OCT-1 has been shown to induce the catalase transcription in human hepatocellular carcinoma cells [55]. On the other hand, the presence of binding sites for the transcriptional factors Sp1, AP1, and nuclear factor kappa B in our promoter prediction indicates the potential transcriptional modulation of RbCat upon exposure to immune signals [56–59].

Fig. 5. Predicted promoter region of rock bream catalase (RbCat) with 5′-untranslated region (UTR) and start codon ATG (bold). The transcription initiation site (+1) is denoted by a curved arrow from which 5′-UTR starts. Anticipated transcription factor binding sites are indicated by bold and underlined letters with their corresponding identity. To distinguish the closely positioned binding sites of nuclear factor kappa B and cAMP-response element binding protein 2, the binding site of cAMP-response element binding protein 2 is additionally shaded in gray color.

3.4. Protein expression and purification of rRbCat

After cloning the coding sequence of RbCat into the pMAL-c2X vector, RbCat was overexpressed as a fusion protein of MBP and purified as described in the Materials and method section. Fractions collected at different stages during the purification steps were visualized by SDS-PAGE (Fig. 6). The purified fusion rRbCat appeared as 2 bands, from which one (102.5 kDa) was detected to be compatible with the predicted size of RbCat (60 kDa) with MBP, since the molecular mass of MBP is 42.5 kDa. However, another band was also appeared below the expected size of the fusion product, probably due to degradation of rRbCat, since vertebrate catalases are known to undergo epigenetic modifications such as proteolysis and form truncated products of the original enzyme [60,61]. This observation is similar to previous reports on the characterization of catalases from invertebrates such as disk abalone, where multiple bands were detected in addition to the expected purified catalase protein band at the respective SDS-PAGE analysis [27].

3.5. Antioxidant activity of rRbCat

Subsequent to the purification step, peroxidase activity of rRbCat against H_2O_2 was evaluated as a function of its concentration. The percent peroxidase activity was plotted against the different rRbCat concentrations used in the experiment (Fig. 7). As expected, the peroxidase activity increased with increasing concentrations of rRbCat, until it reached to a certain threshold level (178.57 μg/mL), exhibiting the optimum peroxidase activity (~94%). This threshold level of rRbCat indicates its optimal concentration for the catalysis of the peroxidase reaction under the

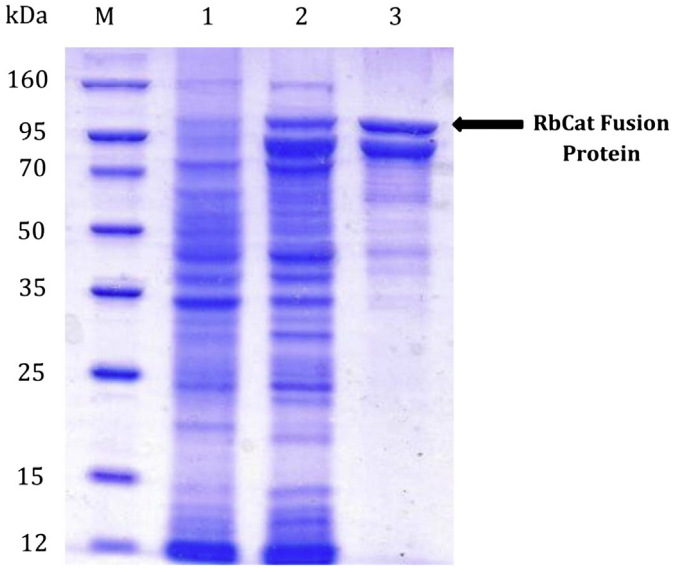

Fig. 6. Sodium dodecyl sulfate-polyacrylamide gel electrophoresis analysis of over-expressed and purified recombinant rock bream catalase (rRbCat) fusion protein. Lane 1, total cellular extract from *Escherichia coli* BL21 (DE3) carrying the rRbCat-MBP expression vector prior to isopropyl-β-galactopyranoside (IPTG) induction; 2, crude extract of rRbCat fusion; 3, purified recombinant fusion protein (rRbCat-MBP) after IPTG induction (1 mM); 4, protein marker (Enzynomics – Korea).

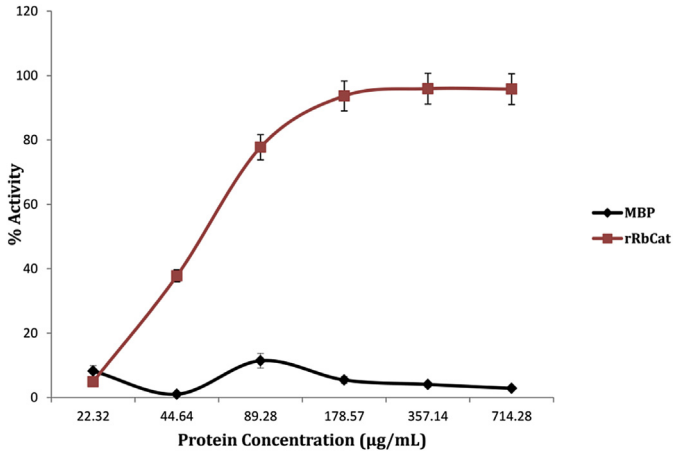

Fig. 7. *In vitro* peroxidase activity of recombinant rock bream catalase (rRbCat) fusion protein against its substrate hydrogen peroxide at different concentrations. Error bars represent the SD ($n = 3$).

provided conditions. Thereafter, the activity of rRbCat was detected to be almost stable with increasing concentration, as evidenced by a plateau shape of the graph. However, the percent peroxidase activity exhibited by MBP against the same substrate, H_2O_2, was found to be negligible compared to the reported activity of the rRbCat fusion protein, especially with increased concentrations of the fusion protein, affirming that the MBP portion of the fusion product did not noticeably affect the overall peroxidase activity. The estimated specific activity of rRbCat using the detected optimal concentration of the enzyme was around 2320 U/mg, which is more or less compatible with the specific activity value obtained for the recombinant catalase enzyme of zebrafish (3160 U/mg) [26].

3.6. Biochemical properties of rRbCat

In order to understand the favorable reaction conditions for rRbCat catalysis, its relative activity was evaluated over a range of different pH and temperature conditions. As shown in Fig. 8, rRbCat showed a substantial percent activity, (over 80%) under a wide range of temperatures. The relative enzymatic activity from 10 °C to 37 °C varied slightly. Subsequently, the activity was found to decrease slightly from 37 °C to 60 °C and came to a plateau at 70 °C and 80 °C. Altogether, overall percent activity of RbCat was maintained almost constantly, without any considerable variation within the experimental range of temperatures. This observation was not unlike with our previous observation of abalone catalase, in which activity was found to be constant from 30 °C to 70 °C [27]. Our observation of prominent activity of RbCat maintained at even higher temperatures may be attributed with its specific arrangement of β-barrel domain with anti-parallel β sheets, which was already known to support for the higher activity of catalase at increased temperatures, as reported previously [62]. However, MBP alone did not show any significant activity compared to rRbCat under any temperature condition provided, suggesting its inert behavior in the rRbCat fusion protein.

Recombinant RbCat catalyzed the substrate H_2O_2 efficiently, showing a relative activity within the range of 80%–100% over a broad pH spectrum, as shown in the plotted graph of its relative activity under different pH conditions; however, a small but noticeable decrease in its activity was observed at pH 5.5 (~86% activity) (Fig. 9). The maximum percent activity (~96%–97%) laid at pH 6.5–pH 7.5, suggesting that this is the optimal pH for the catalytic reaction under provided conditions. Nevertheless, from pH 7.5 to 8.5, a slight decrease in the RbCat activity was observed. Similarly, chicken catalase also exerted substantial activity within a broad pH range (4–10) [63]. Furthermore, the detected optimal pH range for human catalase (6.8–7.5) [64] and chicken catalase (6–8) [63] is similar to the optimal pH range of rRbCat, further lying within the acceptable pH range (4–11) of various catalases from different species, as retrieved from the "BRENDA" enzyme information system [65]. Nonetheless, similar to the temperature dependency, MBP did not show any detectable activity within the applied pH range, rendering its dormant behavior in the fusion product.

3.7. Tissue-specific mRNA expression profile of RbCat

According to the tissue-specific mRNA expression in selected tissues of rock bream, RbCat was found to be ubiquitously expressed in tissues examined with the highest transcript level in blood and a moderately high level in liver, compared to the expression level in muscle, which showed the lowest expression level among all tissues used in this comparison (Fig. 10). The detected variable transcript profile in different tissues of rock bream reflects the differential metabolic activity in those tissues with respect to the production of ROS and different environmental conditions. In this regard, ROS production plays a key role as an

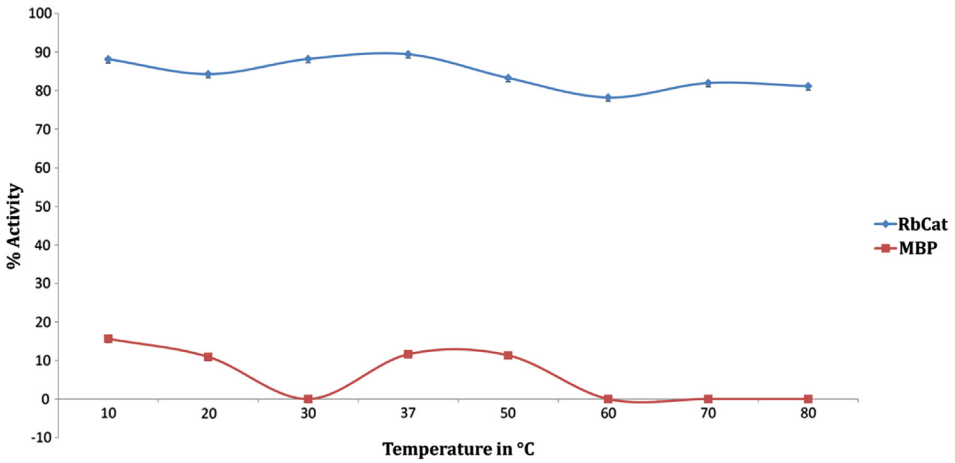

Fig. 8. Variation of recombinant rock bream catalase (rRbCat) peroxidase activity as a function of temperature. Relative enzyme activity percentage (%) was determined at different temperatures ranging from 10 to 80 °C. Error bars represent the SD ($n = 3$).

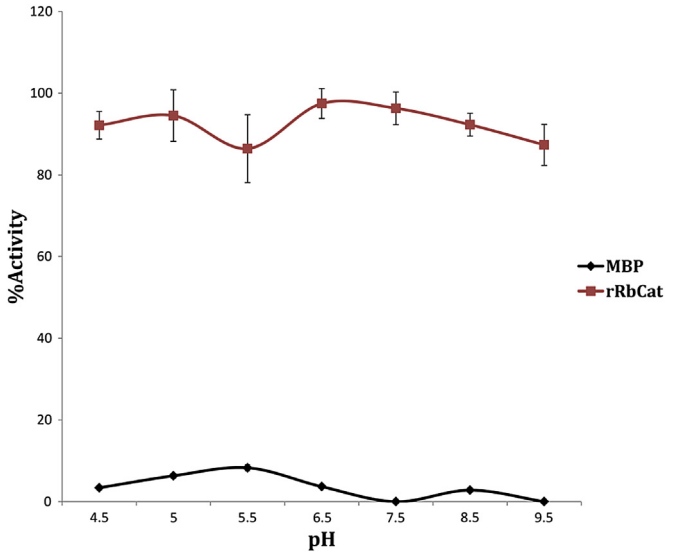

Fig. 9. Variation of recombinant rock bream catalase (rRbCat) peroxidase activity as a function of pH. Relative enzyme activity percentage (%) was determined at different pH conditions, ranging from 4.5 to 9.5. Error bars represent the SD ($n = 3$).

innate immune response during pathogen infections while evacuating foreign invaders by activating immune signaling pathways [66]. On the other hand, for immune reactions such as phagocytosis, blood cells consume high amounts of oxygen for their metabolic functions, which may in turn contribute to the increase of ROS production. Therefore, it is logical to correlate the high levels of catalase-like antioxidant enzyme expression in blood with their antioxidant properties to counterbalance the highly potential overproduction of ROS as a quick response to pathogenic invasion. Furthermore, liver cells frequently undergo oxidative stress, which affects the liver function and induces apoptosis [67]. Therefore, ROS production should be tightly regulated in the liver. Interestingly, our observation of substantial expression of RbCat in liver tissues supports to this fact.

Complying with the pronounced expression of RbCat in liver tissue, catalase transcription was found to be prominent in liver tissues of mefugu (*Takifugu obscurus*) in a previous report [68]. On the other hand, both substantial mRNA and protein expression of zebrafish catalase were detected in its abdominal section. Catalases from Chinese shrimp, *Fenneropenaeus chinensis* [30] and pearl oyster (*Pinctada fucata*) [29] showed their highest expression levels in their intestines, whereas moderately high transcript levels in hemocytes and hepatopancreas with respect to shrimp and in gonad, gill, and mantel regarding oyster.

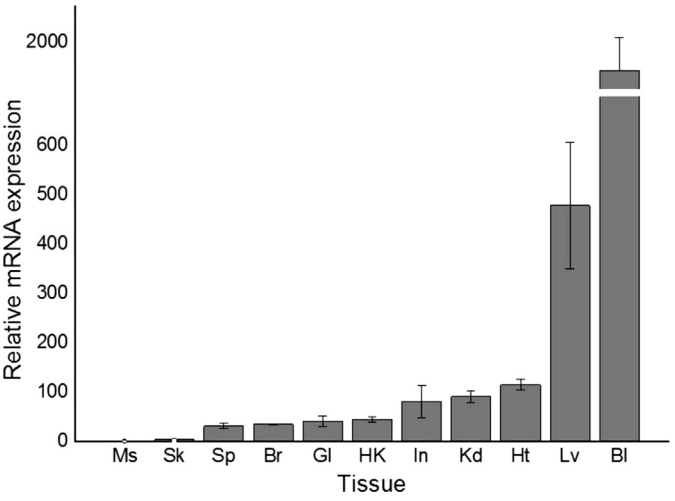

Fig. 10. Tissue-specific expression analysis of rock bream catalase mRNA, determined by quantitative real time-polymerase chain reaction. Expression fold changes are shown relative to the mRNA expression level in muscle tissue. Error bars represent the SD ($n = 3$). Ms – muscle, Sk – skin, Sp – spleen, Br – brain, Gl – gill, HK – head kidney, In – intestine, Kd – kidney, Ht – heart, Lv – liver, and Bl – blood.

3.8. Transcriptional response of RbCat upon immune stimulation

With the objective of evaluating the role of RbCat in the regulation of the cellular redox balance in rock bream upon pathogen infection, its temporal transcriptional variation in blood was investigated under pathological conditions, using two live pathogens, *E. tarda* and RBIV, along with the well-characterized mitogens LPS and poly I:C for immune stimulation. Transcript levels of *RbCat* at each time point after the respective immune stimulation were detected using qRT-PCR. In all qRT-PCR analyses, mRNA expression levels of *RbCat* were detected relative to the corresponding expression of the rock bream *β-actin* gene and further normalized to the corresponding PBS-injected controls at each time point. The relative expression level at the 0 h time point (un-injected control) was used as basal level.

In accordance with graph A in Fig. 11, *RbCat* expression following exposure to *E. tarda* was significantly ($P < 0.05$) elevated

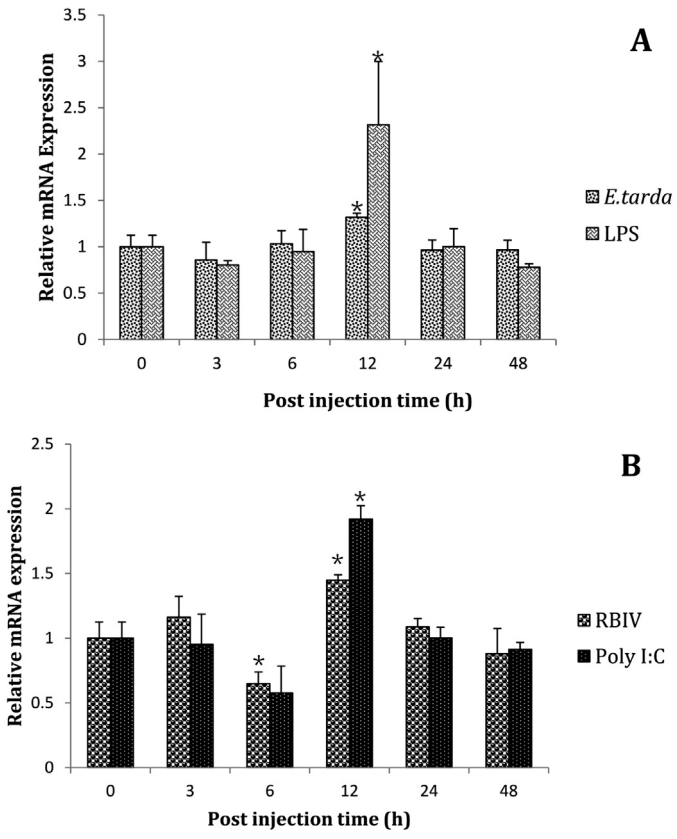

Fig. 11. Expression profile of rock bream catalase mRNA in blood upon immune stimulation with (A) lipopolysaccharide or *Edwardsiella tarda* bacteria, (B) polyinosinic:polycytidylic acid or rock bream iridovirus, as determined by quantitative real time-polymerase chain reaction. The relative expression was calculated by applying the $2^{-\Delta\Delta CT}$ method using rock bream β-actin as reference gene with respect to corresponding phosphate-buffered saline-injected controls at each time point. The relative expression fold change at 0 h post-injection was used as the basal line. Error bars represent the SD ($n = 3$); $^{*}P < 0.05$.

at 12 h post-injection (p.i.), although the fold induction (1.2) was relatively low compared to the un-injected control. However, upon LPS stimulation, the *RbCat* transcript level was significantly ($P < 0.05$) up-regulated with a higher inductive fold change (~2) also at 12 h p.i. (Fig. 11A). The induction at the same time point suggests that LPS may act as a pathogen-associated molecular pattern (PAMP) on *E. tarda*, which triggers the immune response in rock bream, stimulating the production of ROS such as H_2O_2, since LPS is a well-characterized endotoxin of Gram-negative bacteria such as *E. tarda*. Similarly, upon RBIV injection, *RbCat* transcription was significantly ($P < 0.05$) increased at 12 h p.i., exhibiting a low induction fold (1.4) compared to the basal level (Fig. 11B). Further, a significant down-regulation ($P < 0.05$) was also noted at 6 h p.i, under the stress of RBIV. The mitogen poly I:C, which mimics viral dsRNA, boosted its expression by almost 2-fold at 12 h p.i. (Fig. 11B).

According to the overall insights into the immune inductions, mitogen stimulation induced the *RbCat* expression with a higher fold change compared to live pathogen exposure. This observation can be attributed to the immune evasion mechanisms orchestrated by pathogenic organisms, especially bacteria and virus, against the host immune responses, including ROS production [69]. In this regard, intracellular bacteria such as *E. tarda* [70] and some viruses can alter the ROS production; particularly bacteria can reduce ROS production. Therefore, the expression levels of antioxidant enzymes such as catalase may not be dramatically induced upon infection with these bacteria. On the other hand, some viruses such as Japanese encephalitis virus can down-regulate antioxidant enzymes to induce ROS production in host cells and, in turn, induce cell apoptosis, in order to spread the infection to other cells [69,71]. This mechanism used by the virus can be correlated with our observation of down-regulated *RbCat* transcript levels at the early phase of RBIV exposure, where catalase expression may be suppressed by RBIV. Nevertheless, subsequent up-regulation of *RbCat* transcription may be triggered by other immune responses elicited by host cells to control the viral population.

Regarding the antioxidant system in animals, thioredoxin peroxidase and glutathione peroxidase are known to be the predominant antioxidant enzymes involved in the efficient detoxification of H_2O_2 with a higher affinity than catalases, even at a very low concentration of H_2O_2 in cells [72,73]. Moreover, due to the narrow distribution within the cell, and restricted localization into the peroxisomes, catalases can only act on H_2O_2 after H_2O_2 diffused into peroxisomes and when its concentration reached a substantial level. Therefore, ROS production at the early stage of pathogen infection may be counterbalanced by thioredoxin peroxidase and glutathione peroxidase, instead of catalase, which is reflected through the detected transcriptional variation of RbCat under pathological conditions.

The temporal transcription pattern of RbCat upon RBIV exposure does not show any significantly variation from the overall transcriptional response of its invertebrate counterpart of *F. chinensis*, upon white spot syndrome virus stimulation. Therein, transcriptional down-regulation was observed at the early phase while significant ($P < 0.05$) up-regulation was observed in the later phase, both in hemocytes and hepatopancreas [30]. Moreover, temporal transcriptional induction of RbCat under *E. tarda* and LPS exposure can be correlated with the mRNA expression pattern of *Chlamys farreri* in hemocytes after *Vibrio anguillarum* infection, showing up-regulated transcript levels at 12 h p.i. [28]. This is in contrast with the changes in the mRNA expression pattern of its invertebrate counterpart of pearl oyster in intestine following challenge with *Vibrio alginolyticus*, where transcription was up-regulated at the early phase as well as at the late phase of the experiment [29].

4. Conclusion

In conclusion, a novel catalase counterpart from rock bream was identified and characterized at genomic, transcriptional, and protein levels, and its biochemical properties were analyzed as a function of different environmental factors. According to genomic sequence studies, *RbCat* was found to be a multi-exonic gene, in which most of the exons are highly conserved among vertebrates. The *in-silico* predicted core promoter region of *RbCat* reflected its significant regulation at the transcriptional level, especially upon exposure to immune signals and signals generated by oxidative agents. With respect to molecular characterization and phylogenetic analysis, RbCat was positioned with known counterparts of other vertebrates, particularly with teleosts. Constitutive *RbCat* mRNA expression was detected in a tissue-specific manner, suggesting its diverse importance in the physiology with respect to the tissue type. Moreover, *RbCat* transcription was differently modulated upon exposure to four different immune stimulants, suggesting its potential role as an antioxidative enzyme in post-immune responses at the protein level. Recombinant RbCat demonstrated detectable peroxidase activity against H_2O_2 in a dose-dependent manner, affirming its functional viability, while it exhibited substantial activity under a broad range of temperatures and pH conditions. However, this study can be further extended to examine RbCat with respect to its potential functional properties in fish physiology.

Acknowledgments

This research was supported by Basic Science Research Program through the National Research Foundation of Korea (NRF) funded by the Ministry of Education, Science and Technology.

References

[1] Buonocore G, Perrone S, Tataranno ML. Oxygen toxicity: chemistry and biology of reactive oxygen species. Seminars in Fetal & Neonatal Medicine 2010;15:186–90.
[2] Nordberg J, Arner ES. Reactive oxygen species, antioxidants, and the mammalian thioredoxin system. Free Radical Biology & Medicine 2001;31:1287–312.
[3] Arnoult D, Soares F, Tattoli I, Castanier C, Philpott DJ, Girardin SE. An N-terminal addressing sequence targets NLRX1 to the mitochondrial matrix. Journal of Cell Science 2009;122:3161–8.
[4] Moore CB, Bergstralh DT, Duncan JA, Lei Y, Morrison TE, Zimmermann AG, et al. NLRX1 is a regulator of mitochondrial antiviral immunity. Nature 2008;451:573–7.
[5] Groeger G, Quiney C, Cotter TG. Hydrogen peroxide as a cell-survival signaling molecule. Antioxidants & Redox Signaling 2009;11:2655–71.
[6] Leto TL, Morand S, Hurt D, Ueyama T. Targeting and regulation of reactive oxygen species generation by Nox family NADPH oxidases. Antioxidants & Redox Signaling 2009;11:2607–19.
[7] Circu ML, Aw TY. Reactive oxygen species, cellular redox systems, and apoptosis. Free Radical Biology & Medicine 2010;48:749–62.
[8] Morey M, Serras F, Baguna J, Hafen E, Corominas M. Modulation of the Ras/MAPK signalling pathway by the redox function of selenoproteins in *Drosophila melanogaster*. Developmental Biology 2001;238:145–56.
[9] Nakano H, Nakajima A, Sakon-Komazawa S, Piao JH, Xue X, Okumura K. Reactive oxygen species mediate crosstalk between NF-kappaB and JNK. Cell Death and Differentiation 2006;13:730–7.
[10] Forman HJ, Maiorino M, Ursini F. Signaling functions of reactive oxygen species. Biochemistry 2010;49:835–42.
[11] Kowaltowski AJ, de Souza-Pinto NC, Castilho RF, Vercesi AE. Mitochondria and reactive oxygen species. Free Radical Biology & Medicine 2009;47:333–43.
[12] Wang C, Yue X, Lu X, Liu B. The role of catalase in the immune response to oxidative stress and pathogen challenge in the clam *Meretrix meretrix*. Fish & Shellfish Immunology 2013;34:91–9.
[13] Abele D, Puntarulo S. Formation of reactive species and induction of antioxidant defence systems in polar and temperate marine invertebrates and fish. Comparative Biochemistry and Physiology Part A, Molecular & Integrative Physiology 2004;138:405–15.
[14] Ha EM, Oh CT, Ryu JH, Bae YS, Kang SW, Jang IH, et al. An antioxidant system required for host protection against gut infection in Drosophila. Developmental Cell 2005;8:125–32.

[15] Nicholls P. Classical catalase: ancient and modern. Archives of Biochemistry and Biophysics 2012;525:95–101.
[16] Oshino N, Chance B, Sies H, Bucher T. The role of H_2O_2 generation in perfused rat liver and the reaction of catalase compound I and hydrogen donors. Archives of Biochemistry and Biophysics 1973;154:117–31.
[17] Kashiwagi A, Kashiwagi K, Takase M, Hanada H, Nakamura M. Comparison of catalase in diploid and haploid *Rana rugosa* using heat and chemical inactivation techniques. Comparative Biochemistry and Physiology Part B, Biochemistry & Molecular Biology 1997;118:499–503.
[18] Klotz MG, Klassen GR, Loewen PC. Phylogenetic relationships among prokaryotic and eukaryotic catalases. Molecular Biology and Evolution 1997;14:951–8.
[19] Mackay WJ, Bewley GC. The genetics of catalase in *Drosophila melanogaster*: isolation and characterization of acatalasemic mutants. Genetics 1989;122:643–52.
[20] Bryant DD, Wilson GN. Differential evolution and expression of murine peroxisomal membrane protein genes. Biochemical and Molecular Medicine 1995;55:22–30.
[21] McClung CR. Regulation of catalases in Arabidopsis. Free Radical Biology & Medicine 1997;23:489–96.
[22] Storz G, Tartaglia LA. OxyR: a regulator of antioxidant genes. The Journal of Nutrition 1992;122:627–30.
[23] Yamamoto K, Banno Y, Fujii H, Miake F, Kashige N, Aso Y. Catalase from the silkworm, *Bombyx mori*: gene sequence, distribution, and overexpression. Insect Biochemistry and Molecular Biology 2005;35:277–83.
[24] Putnam CD, Arvai AS, Bourne Y, Tainer JA. Active and inhibited human catalase structures: ligand and NADPH binding and catalytic mechanism. Journal of Molecular Biology 2000;296:295–309.
[25] Gerhard GS, Kauffman EJ, Grundy MA. Molecular cloning and sequence analysis of the *Danio rerio* catalase gene. Comparative Biochemistry and Physiology Part B, Biochemistry & Molecular Biology 2000;127:447–57.
[26] Ken CF, Lin CT, Wu JL, Shaw JF. Cloning and expression of a cDNA coding for catalase from zebrafish (*Danio rerio*). Journal of Agricultural and Food Chemistry 2000;48:2092–6.
[27] Ekanayake PM, De Zoysa M, Kang HS, Wan Q, Jee Y, Lee YH, et al. Cloning, characterization and tissue expression of disk abalone (*Haliotis discus discus*) catalase. Fish & Shellfish Immunology 2008;24:267–78.
[28] Li C, Ni D, Song L, Zhao J, Zhang H, Li L. Molecular cloning and characterization of a catalase gene from Zhikong scallop *Chlamys farreri*. Fish & Shellfish Immunology 2008;24:26–34.
[29] Guo H, Zhang D, Cui S, Chen M, Wu K, Li Y, et al. Molecular characterization and mRNA expression of catalase from pearl oyster *Pinctada fucata*. Marine Genomics 2011;4:245–51.
[30] Zhang Q, Li F, Zhang X, Dong B, Zhang J, Xie Y, et al. cDNA cloning, characterization and expression analysis of the antioxidant enzyme gene, catalase, of Chinese shrimp *Fenneropenaeus chinensis*. Fish & Shellfish Immunology 2008;24:584–91.
[31] Oh MJ, Kitamura SI, Kim WS, Park MK, Jung SJ, Miyadai T, et al. Susceptibility of marine fish species to a megalocytivirus, turbot iridovirus, isolated from turbot, *Psetta maximus* (L.). Journal of Fish Diseases 2006;29:415–21.
[32] Li H, Sun ZP, Li Q, Jiang YL. Characterization of an iridovirus detected in rock bream (*Oplegnathus fasciatus*; Temminck and Schlegel). Bing du xue bao = Chinese Journal of Virology/[bian ji, Bing du xue bao bian ji wei yuan hui] 2011;27:158–64.
[33] Park SL. Disease control in Korean aquaculture. Journal of Fish Pathology 2006;44:19–23.
[34] Tort L. Stress and immune modulation in fish. Developmental and Comparative Immunology 2011;35:1366–75.
[35] Whang I, Lee Y, Kim H, Jung SJ, Oh MJ, Choi CY, et al. Characterization and expression analysis of the myeloid differentiation factor 88 (MyD88) in rock bream *Oplegnathus fasciatus*. Molecular Biology Reports 2011;38:3911–20.
[36] Quiniou SM, Katagiri T, Miller NW, Wilson M, Wolters WR, Waldbieser GC. Construction and characterization of a BAC library from a gynogenetic channel catfish *Ictalurus punctatus*. Genetics, Selection, Evolution: GSE 2003;35:673–83.
[37] Tamura K, Dudley J, Nei M, Kumar S. MEGA4: molecular evolutionary genetics analysis (MEGA) software version 4.0. Molecular Biology and Evolution 2007;24:1596–9.
[38] Marchler-Bauer A, Anderson JB, Chitsaz F, Derbyshire MK, DeWeese-Scott C, Fong JH, et al. CDD: specific functional annotation with the conserved domain database. Nucleic Acids Research 2009;37:D205–10.
[39] Zhang Y. I-TASSER server for protein 3D structure prediction. BMC Bioinformatics 2008;9:40.
[40] Roy A, Kucukural A, Zhang Y. I-TASSER: a unified platform for automated protein structure and function prediction. Nature Protocols 2010;5:725–38.
[41] Goodsell DS. Representing structural information with RasMol. Current Protocols in Bioinformatics/Editorial Board, Andreas D Baxevanis [et al]; 2005 [Chapter 5, Unit 5 4].
[42] Reese MG. Application of a time-delay neural network to promoter annotation in the *Drosophila melanogaster* genome. Computers & Chemistry 2001;26:51–6.
[43] Umasuthan N, Whang I, Kim JO, Oh MJ, Jung SJ, Choi CY, et al. Rock bream (*Oplegnathus fasciatus*) serpin, protease nexin-1: transcriptional analysis and characterization of its antiprotease and anticoagulant activities. Developmental and Comparative Immunology 2011;35:785–98.
[44] Bradford MM. A rapid and sensitive method for the quantitation of microgram quantities of protein utilizing the principle of protein-dye binding. Analytical Biochemistry 1976;72:248–54.
[45] Muller HE. Detection of hydrogen peroxide produced by microorganisms on an ABTS peroxidase medium. Zentralblatt fur Bakteriologie, Mikrobiologie, und Hygiene Series A, Medical Microbiology, Infectious Diseases, Virology, Parasitology 1985;259:151–4.
[46] Whang I, Lee Y, Lee S, Oh MJ, Jung SJ, Choi CY, et al. Characterization and expression analysis of a goose-type lysozyme from the rock bream *Oplegnathus fasciatus*, and antimicrobial activity of its recombinant protein. Fish & Shellfish Immunology 2011;30:532–42.
[47] Livak KJ, Schmittgen TD. Analysis of relative gene expression data using real-time quantitative PCR and the 2(−Delta Delta C(T)) method. Methods 2001;25:402–8.
[48] Scibior D, Czeczot H. Catalase: structure, properties, functions. Postepy Higieny i Medycyny Doswiadczalnej 2006;60:170–80.
[49] Moreira SF, Bailao AM, Barbosa MS, Jesuino RS, Felipe MS, Pereira M, et al. Monofunctional catalase P of *Paracoccidioides brasiliensis*: identification, characterization, molecular cloning and expression analysis. Yeast 2004;21:173–82.
[50] Chelikani P, Fita I, Loewen PC. Diversity of structures and properties among catalases. Cellular and Molecular Life Sciences: CMLS 2004;61:192–208.
[51] Modrek B, Lee C. A genomic view of alternative splicing. Nature Genetics 2002;30:13–9.
[52] Black DL. Protein diversity from alternative splicing: a challenge for bioinformatics and post-genome biology. Cell 2000;103:367–70.
[53] Nenoi M, Ichimura S, Mita K, Yukawa O, Cartwright IL. Regulation of the catalase gene promoter by Sp1, CCAAT-recognizing factors, and a WT1/Egr-related factor in hydrogen peroxide-resistant HP100 cells. Cancer Research 2001;61:5885–94.
[54] Taniguchi M, Hashimoto M, Hori N, Sato K. CCAAT/enhancer binding protein-beta (C/EBP-beta), a pivotal regulator of the TATA-less promoter in the rat catalase gene. FEBS Letters 2005;579:5785–90.
[55] Quan X, Lim SO, Jung G. Reactive oxygen species downregulate catalase expression via methylation of a CpG island in the Oct-1 promoter. FEBS Letters 2011;585:3436–41.
[56] Lacroix I, Lipcey C, Imbert J, Kahn-Perles B. Sp1 transcriptional activity is up-regulated by phosphatase 2A in dividing T lymphocytes. The Journal of Biological Chemistry 2002;277:9598–605.
[57] Parrott C, Seidner T, Duh E, Leonard J, Theodore TS, Buckler-White A, et al. Variable role of the long terminal repeat Sp1-binding sites in human immunodeficiency virus replication in T lymphocytes. Journal of Virology 1991;65:1414–9.
[58] Hess J, Angel P, Schorpp-Kistner M. AP-1 subunits: quarrel and harmony among siblings. Journal of Cell Science 2004;117:5965–73.
[59] Tian B, Brasier AR. Identification of a nuclear factor kappa B-dependent gene network. Recent Progress in Hormone Research 2003;58:95–130.
[60] Crane D, Holmes R, Masters C. Proteolytic modification of mouse liver catalase. Biochemical and Biophysical Research Communications 1982;104:1567–72.
[61] Sun Y. Multiplicity of antioxidant enzyme catalase in mouse liver cells. Free Radical Research 1997;26:343–50.
[62] Murthy MR, Reid 3rd TJ, Sicignano A, Tanaka N, Rossmann MG. Structure of beef liver catalase. Journal of Molecular Biology 1981;152:465–99.
[63] Aydemir T, Kuru K. Purification and partial characterization of catalase from chicken erythrocytes and the effect of various inhibitors on enzyme activity. Turkish Journal of Chemistry 2003;27:85–98.
[64] Aebi H. Catalase in vitro. Methods in Enzymology 1984;105:121–6.
[65] Scheer M, Grote A, Chang A, Schomburg I, Munaretto C, Rother M, et al. BRENDA, the enzyme information system in 2011. Nucleic Acids Research 2011;39:D670–6.
[66] Kohchi C, Inagawa H, Nishizawa T, Soma G. ROS and innate immunity. Anticancer Research 2009;29:817–21.
[67] Kamata H, Honda S, Maeda S, Chang L, Hirata H, Karin M. Reactive oxygen species promote TNFalpha-induced death and sustained JNK activation by inhibiting MAP kinase phosphatases. Cell 2005;120:649–61.
[68] Kim JH, Rhee JS, Lee JS, Dahms HU, Lee J, Han KN, et al. Effect of cadmium exposure on expression of antioxidant gene transcripts in the river pufferfish, *Takifugu obscurus* (Tetraodontiformes). Comparative Biochemistry and Physiology Toxicology & Pharmacology: CBP 2010;152:473–9.
[69] Borjesson DL, Kobayashi SD, Whitney AR, Voyich JM, Argue CM, Deleo FR. Insights into pathogen immune evasion mechanisms: *Anaplasma phagocytophilum* fails to induce an apoptosis differentiation program in human neutrophils. Journal of Immunology 2005;174:6364–72.
[70] Ling SH, Wang XH, Xie L, Lim TM, Leung KY. Use of green fluorescent protein (GFP) to study the invasion pathways of *Edwardsiella tarda* in in vivo and in vitro fish models. Microbiology 2000;146(Pt 1):7–19.
[71] Yang TC, Lai CC, Shiu SL, Chuang PH, Tzou BC, Lin YY, et al. Japanese encephalitis virus down-regulates thioredoxin and induces ROS-mediated ASK1-ERK/p38 MAPK activation in human promonocyte cells. Microbes and Infection/Institut Pasteur 2010;12:643–51.
[72] Jang HH, Lee KO, Chi YH, Jung BG, Park SK, Park JH, et al. Two enzymes in one; two yeast peroxiredoxins display oxidative stress-dependent switching from a peroxidase to a molecular chaperone function. Cell 2004;117:625–35.
[73] Kang SW, Rhee SG, Chang TS, Jeong W, Choi MH. 2-Cys peroxiredoxin function in intracellular signal transduction: therapeutic implications. Trends in Molecular Medicine 2005;11:571–8.